

Oxygen binding by $\alpha(\text{Fe}^{2+})_2\beta(\text{Ni}^{2+})_2$ hemoglobin crystals

STEFANO BRUNO,¹ STEFANO BETTATI,¹ MICHELE MANFREDINI,¹ ANDREA MOZZARELLI,^{1,2}
MARTINO BOLOGNESI,³ DANIELA DERIU,³ CAMILLO ROSANO,³ ANTONIO TSUNESHIGE,⁴
TAKASHI YONETANI,⁴ AND ERIC R. HENRY⁵

¹Institute of Biochemical Sciences, University of Parma, 43100 Parma, Italy

²National Institute for the Physics of Matter, University of Parma, 43100 Parma, Italy

³Center of Advanced Biotechnology-IST and Department of Physics, National Institute for the Physics of Matter,
University of Genova, 16132 Genova, Italy

⁴Department of Biochemistry and Biophysics, University of Pennsylvania School of Medicine, Philadelphia, Pennsylvania 19104

⁵Laboratory of Chemical Physics, NIDDK, NIH, Bethesda, Maryland 20892

(RECEIVED November 11, 1999; FINAL REVISION January 12, 2000; ACCEPTED February 11, 2000)

Abstract

Oxygen binding by hemoglobin fixed in the T state either by crystallization or by encapsulation in silica gels is apparently noncooperative. However, cooperativity might be masked by different oxygen affinities of α and β subunits. Metal hybrid hemoglobins, where the noniron metal does not bind oxygen, provide the opportunity to determine the oxygen affinities of α and β hemes separately. Previous studies have characterized the oxygen binding by $\alpha(\text{Ni}^{2+})_2\beta(\text{Fe}^{2+})_2$ crystals. Here, we have determined the three-dimensional (3D) structure and oxygen binding of $\alpha(\text{Fe}^{2+})_2\beta(\text{Ni}^{2+})_2$ crystals grown from polyethylene glycol solutions. Polarized absorption spectra were recorded at different oxygen pressures with light polarized parallel either to the b or c crystal axis by single crystal microspectrophotometry. The oxygen pressures at 50% saturation (p50s) are 95 ± 3 and 87 ± 4 Torr along the b and c crystal axes, respectively, and the corresponding Hill coefficients are 0.96 ± 0.06 and 0.90 ± 0.03 . Analysis of the binding curves, taking into account the different projections of the α hemes along the optical directions, indicates that the oxygen affinity of α_1 hemes is 1.3-fold lower than α_2 hemes. Inspection of the 3D structure suggests that this inequivalence may arise from packing interactions of the Hb tetramer within the monoclinic crystal lattice. A similar inequivalence was found for the β subunits of $\alpha(\text{Ni}^{2+})_2\beta(\text{Fe}^{2+})_2$ crystals. The average oxygen affinity of the α subunits (p50 = 91 Torr) is about 1.2-fold higher than the β subunits (p50 = 110 Torr). In the absence of cooperativity, this heterogeneity yields an oxygen binding curve of Hb A with a Hill coefficient of 0.999. Since the binding curves of Hb A crystals exhibit a Hill coefficient very close to unity, these findings indicate that oxygen binding by T-state hemoglobin is noncooperative, in keeping with the Monod, Wyman, and Changeux model.

Keywords: allosteric models; hemoglobin crystals; microspectrophotometry; oxygen binding; X-ray crystallography

Several models have been proposed over the years to explain cooperative oxygen binding by hemoglobin (Hb): the Monod, Wyman, and Changeux model (MWC) (Monod et al., 1965), the Pauling model (Pauling, 1935), later expanded by Koshland, Nemethy, and Filmer (KNF) (Koshland et al., 1966), the stereochemical mechanism of Perutz (1970) and the symmetry rules of Ackers et al. (1992). A critical difference among these models is the degree of cooperativity of the T quaternary state and, therefore, the extent of signal communication between hemes. Whereas the MWC model predicts that oxygen binds to both the T and R state noncooperatively and that, therefore, there is no direct heme–heme interaction,

the Pauling–KNF model predicts that oxygen binding to a heme affects both the structure and the affinity of the adjacent subunits. The original stereochemical mechanism of Perutz (1970) focused on the role of salt bridges in the stabilization of a low-affinity T state and in the origin of the Bohr effect. The structural mechanism was fully in agreement with the essential features of the MWC model. Tertiary conformational changes that occur upon oxygen binding within a subunit do not propagate through either the α_1 – β_2 or the α_2 – β_1 interfaces, and there are only two quaternary states. However, in later formulations of his model, Perutz seemed to accept the idea of intersubunit signals (Perutz, 1989; Perutz et al., 1998). Recent X-ray diffraction data on fully oxygenated hemoglobin were interpreted as evidence of such heme–heme interaction (Paoli et al., 1996). Ackers et al. (1992) found that the free energy distribution of the intermediate species formed using cya-

Reprint requests to: Andrea Mozzarelli, Institute of Biochemical Sciences, University of Parma, 43100 Parma, Italy; e-mail: biochim@ipr.univ.cce.unipr.it.

monet hybrids and some metal-hybrid hemoglobins deviates significantly from the predictions of the MWC model (Ackers et al., 1992; Ackers, 1998). To account for these deviations, a model was proposed that requires ligand binding to the T state to be cooperative. The degree of cooperativity strongly depends on the tetrameric hemoglobin used to mimic intermediate states of oxygenation. However, careful studies (Shibayama et al., 1997, 1998) have demonstrated that key results of Ackers's work are affected by valency exchange between deoxy and cyanomethemes. Furthermore, the values of cooperative free energies of the tetramer-dimer dissociation at different degrees of ligation (Ackers, 1998) indicated that the intradimer cooperativity upon oxygen binding is very small compared to that arising from the quaternary transition (Eaton et al., 1999). In a recent analysis, it was concluded that both thermodynamic and kinetic data of ligand binding to hemoglobin are well explained by the MWC model (Eaton et al., 1999). A critical test of the model was the determination of the degree of cooperativity of oxygen binding by the T quaternary state of Hb. A T-state Hb that does not switch to the R state upon exposure to oxygen can be obtained either by crystallization from polyethylene glycol (PEG) solutions (Brzozowski et al., 1984; Mozzarelli et al., 1991), by deoxyHb encapsulation in silica gels (Shibayama & Saigo, 1995; Bettati & Mozzarelli, 1997) or by the substitution of the ferrous iron with nonoxygen binding metal ions, such as nickel (Shibayama et al., 1986a, 1986b). Oxygen binding curves for T-state hemoglobin in the crystalline state as well as in the gel were characterized by a Hill coefficient close to unity, in spite of significant differences in oxygen affinities and Bohr effect (Rivetti et al., 1993a; Shibayama & Saigo, 1995; Bettati & Mozzarelli, 1997; Mozzarelli et al., 1997). However, a Hill coefficient of unity could occur in the presence of cooperativity that is compensated, and therefore masked, by the inequivalence of the oxygen affinities of the α and β subunits (Rivetti et al., 1993a; Eaton et al., 1999). Rivetti et al. (1993a) calculated that the α subunits bind oxygen with an affinity four- to fivefold higher than the β subunits. Consequently, the estimated cooperative free energy of binding within the T quaternary state was $\sim 10\%$ of the overall cooperative binding free energy, as measured by the difference in binding free energy of the first and fourth oxygen molecules. The calculations were based on the different projections of α and β hemes along the crystal axes derived from the three-dimensional (3D) structure of the unliganded and liganded Hb. At that time, the structure of the fully oxygenated Hb was not available and was obtained by combining the structure of the α -oxyHb (Liddington et al., 1988, 1992) with that of the $\alpha(\text{Ni}^{2+})_2\beta(\text{Fe}^{2+}\text{CO})_2$ (Luisi et al., 1990). Recently, by using oxygen binding curves of Hb in the presence of inositol hexaphosphate and the corresponding structures of the deoxygenated and fully oxygenated Hb in the presence of the allosteric effector (Paoli et al., 1996), the calculated $\alpha\beta$ inequivalence was found to be 2.5 (Mozzarelli et al., 1997). To experimentally determine the difference of oxygen affinity between the α and β subunits, an investigation of $\alpha(\text{Ni}^{2+})_2\beta(\text{Fe}^{2+})_2$ crystals, where Ni-containing hemes do not bind oxygen, was carried out (Bettati et al., 1996). This study indicated that the affinity of the β subunits was about twofold higher than that previously estimated on the basis of the calculations, thus indicating that even the small cooperativity of T-state Hb might be overestimated (Rivetti et al., 1993a; Mozzarelli et al., 1997). Further characterization of the $\alpha\beta$ inequivalence of T state Hb requires the determination of oxygen binding curves for $\alpha(\text{Fe}^{2+})_2\beta(\text{Ni}^{2+})_2$ crystals as well. Crystals of $\alpha(\text{Fe}^{2+})_2\beta(\text{Ni}^{2+})_2$, grown from ammonium sulfate solutions, are

monoclinic and isomorphous to Hb A crystals (Luisi & Shibayama, 1989). However, hemoglobin function in the crystal (Rivetti et al., 1993a, 1993b; Kavanaugh et al., 1995; Bettati et al., 1996, 1997, 1998) and the high-resolution structures of unliganded and liganded Hb (Brzozowski et al., 1984; Liddington et al., 1988, 1992; Paoli et al., 1996) have been determined using crystals grown from PEG solutions. These crystals are particularly stable and do not shatter upon oxygenation, in contrast to the behavior of crystals of hemoglobin grown from high-salt solutions (Haurowitz, 1938). For these reasons, in the present work, crystals of $\alpha(\text{Fe}^{2+})_2\beta(\text{Ni}^{2+})_2$ from PEG solutions were grown, precise oxygen-binding curves were measured and the 3D structure of the deoxygenated species was determined. The results further strengthen the view that T-state hemoglobin binds oxygen noncooperatively.

Results

Three-dimensional structure of deoxy $\alpha(\text{Fe}^{2+})_2\beta(\text{Ni}^{2+})_2$

Inspection of the electron density maps of the refined model in the molecular regions that mostly vary in the T \rightarrow R transition, hydrogen bonds and salt links at the $\alpha_1\beta_2$ and $\alpha_2\beta_1$ interfaces, and the switch region between the C helix of the α chains and the FG corner of the β chains, shows that the crystallized $\alpha(\text{Fe}^{2+})_2\beta(\text{Ni}^{2+})_2$ is in the T quaternary state. Moreover, inspection of the distal site region (Fig. 1) shows that only a weak electron density peak is present in the neighborhood of the α hemes, at 3.4 Å (average for the two α hemes) from the iron atom and, therefore, not coordinated to it. This feature, which was completely absent at the distal site in the β chains, has been interpreted as a distal-site trapped water molecule. As in the other IHP-containing structures of Hb (Paoli et al., 1996), no electron density was observed for the allosteric effector.

A structural overlay of the refined structure with the atomic coordinates of human deoxyHb A, crystallized and solved at the same resolution from PEG solutions in an orthorhombic space group (Protein Data Bank (PDB) data set 1HGA) (Liddington et al., 1992), shows a strong conservation of the 3D structures in the two crystal forms (root-mean-square deviation (RMSD) for the whole tetramer C α backbone is 0.59 Å), the largest deviation being localized at residue Ser D84 (1.83 Å). Similarly, the refined structure of $\alpha(\text{Fe}^{2+})_2\beta(\text{Ni}^{2+})_2$ was compared with those of hybrid Hb crystals grown from high-salt solutions, which display an identical molecular packing in the P2₁ monoclinic crystal lattice. If the complete tetramer structures (570 backbone C α atoms) are superimposed, RMSD values of 0.52 and 0.59 Å are obtained for the comparisons of deoxy $\alpha(\text{Fe}^{2+})_2\beta(\text{Co}^{2+})_2$ and $\alpha(\text{Ni}^{2+})_2\beta(\text{FeCO})_2$, respectively, with the $\alpha(\text{Fe}^{2+})_2\beta(\text{Ni}^{2+})_2$ structure reported here. Table 1 summarizes pairwise structural comparisons for the isolated Hb chains, which underline a substantial structural identity, within the limits of the experimental error, for the hybrid Hb structures, both for salt- and PEG-grown crystals. Within this pattern, the largest structural deviation observed between the $\alpha(\text{Ni}^{2+})_2\beta(\text{Fe}^{2+})_2$ (salt) and the $\alpha(\text{Fe}^{2+})_2\beta(\text{Ni}^{2+})_2$ (PEG) 3D structures occurs in the N-terminal region of the β_2 chain, residue His2 (2.4 Å).

Oxygen binding by $\alpha(\text{Fe}^{2+})_2\beta(\text{Ni}^{2+})_2$ crystals

Polarized absorption spectra were recorded between 0 and 760 Torr of oxygen at 15 °C (Fig. 2). The strong and oxygen-independent

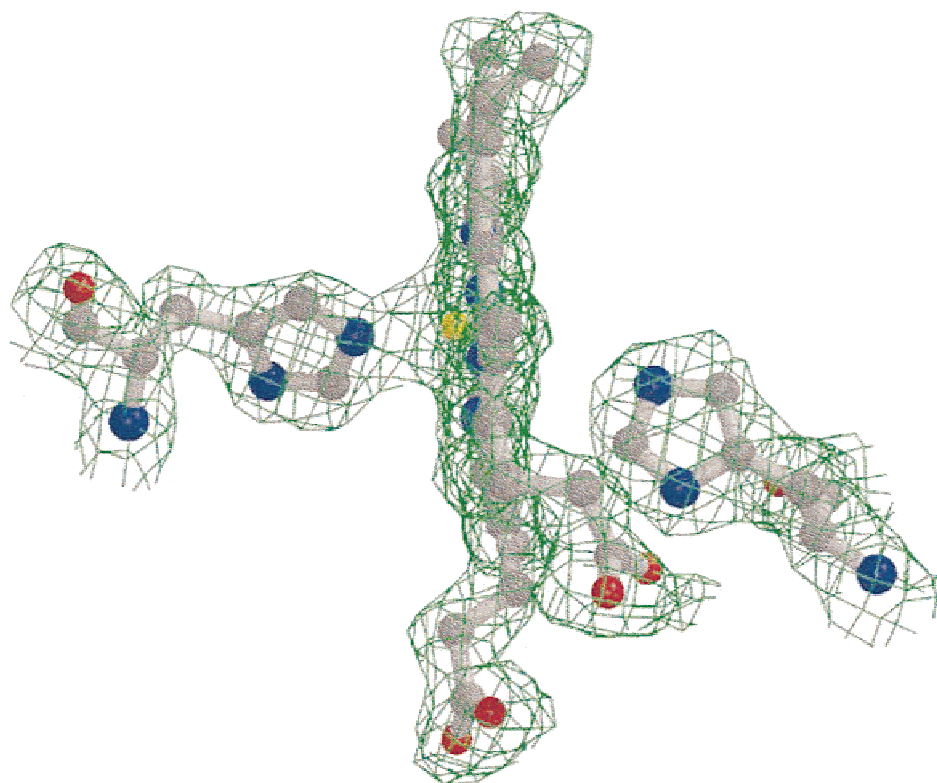


Fig. 1. Electron density map of the α heme of $\alpha(\text{Fe}^{2+})_2\beta(\text{Ni}^{2+})_2$. Electron density is contoured at 1.0σ . The heme group is shown edge-on, from the solvent side of the molecule. The distal HisF7 residue is on the right.

contribution of Ni-porphyrin to the spectra leads to relatively limited spectral changes induced by oxygen binding with respect to those observed for Hb A. Nevertheless, these changes are larger than those observed for $\alpha(\text{Ni}^{2+})_2\beta(\text{Fe}^{2+})_2$ where Ni-porphyrin absorptions strongly dominate the spectra (Bettati et al., 1996). Representative fits of spectra, recorded at different oxygen pressures, to a linear combination of the reference spectra are shown in Figure 3. The calculated fractional saturations with oxygen and the fractions of oxidized hemes are reported in Figure 4. The p50s (the oxygen pressures at half saturation) are 95 ± 3 and 87 ± 4 Torr along the *b* and *c* crystal axes, respectively, indicating that there is a small inequivalence of oxygen affinity between the α hemes. The value of p50 calculated by Rivetti et al. (1993a) for α hemes in Hb A crystals was 80 Torr. The value of p50 determined for the β hemes in $\alpha(\text{Ni}^{2+})_2\beta(\text{Fe}^{2+})_2$ crystals was 110 Torr (Bettati et al.,

1996). The Hill plots (Fig. 5) exhibit slopes of 0.96 ± 0.06 and 0.90 ± 0.03 for the *b* and *c* axes, respectively, indicating that oxygen binding is noncooperative. A Hill *n* lower than one might arise from a difference between the oxygen affinities of α_1 and α_2 due to different intermolecular contacts of the α subunits within the crystal lattice (see Discussion). The projections of heme planes along the optical axes computed from X-ray structures for the oxidized and the oxygenated and deoxygenated reduced forms of $\alpha(\text{Fe}^{2+})_2\beta(\text{Ni}^{2+})_2$ (Table 2; Fig. 6) are used in a procedure described previously (Rivetti et al., 1993a; Bettati et al., 1996) to determine the relations between apparent crystal binding curves and subunit binding curves (Fig. 7). The observed ratio of oxygen affinities along the *b* and *c* axes is 1.09, consistent with a ratio of the p50s of α_1 and α_2 of 1.30 (Fig. 7A) and a calculated Hill *n* greater than 0.999 (Fig. 7B).

Table 1. RMSD values (\AA) calculated in structural overlays of $\alpha(\text{Fe}^{2+})_2\beta(\text{Ni}^{2+})_2$ structure (crystals grown from PEG) with selected liganded and unliganded Hbs^a

Hemoglobin	α Chains (141 C α pairs)	β Chains (144 C α pairs)	Full tetramer (570 C α pairs)	PDB file
$\alpha(\text{Ni}^{2+})_2\beta(\text{Fe}^{2+}\text{CO})_2$	0.38 (1.40)	0.44 (1.14)	0.52 (2.37)	1NIH
$\alpha(\text{Fe}^{2+}\text{CO})_2\beta(\text{Ni}^{2+})_2$	0.34 (1.50)	0.49 (1.47)	0.59 (1.73)	1COH
$\alpha(\text{Fe}^{2+})_2\beta(\text{Fe}^{2+})_2$	0.40 (1.68)	0.45 (1.31)	0.59 (1.83)	1HGA

^aValues in parentheses represent the largest atom deviation observed in each structural comparison.

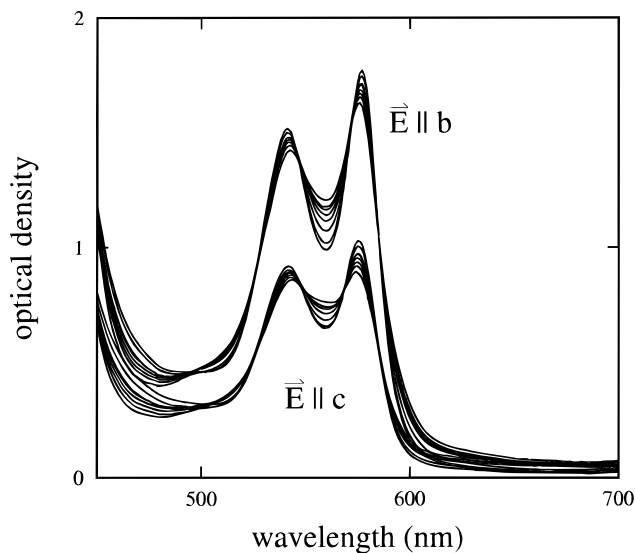


Fig. 2. Polarized absorption spectra of $\alpha(\text{Fe}^{2+})_2\beta(\text{Ni}^{2+})_2$ Hb crystals as a function of oxygen pressure. Crystals were suspended in a solution containing 50% (w/v) PEG 1000, 10 mM potassium phosphate, 1 mM IHP, pH 7, 15 °C, and equilibrated with decreasing oxygen pressures between 760 and 0 Torr. Polarized absorption spectra were collected with light linearly polarized parallel to either the *b* or the *c* axis.

Inter- and intra-subunit salt bridges are involved in the control of T-state oxygen affinity as well as in T-state quaternary stabilization (Perutz, 1970; Sun et al., 1997). The oxygen affinity of T-state Hb increases as pH increases (tertiary Bohr effect) (Lee et al., 1988). We have measured the oxygen binding by $\alpha(\text{Fe}^{2+})_2\beta(\text{Ni}^{2+})_2$ as a function of pH. It was found that the oxygen affinity is pH-independent (Fig. 8), as observed for Hb A and $\alpha(\text{Ni}^{2+})_2\beta(\text{Fe}^{2+})_2$ crystals (Rivetti et al., 1993a; Bettati et al., 1996). $\alpha(\text{Fe}^{2+})_2\beta(\text{Ni}^{2+})_2$ binds oxygen noncooperatively in solution, with a pH-dependent $p50$ that has a value of ~ 170 Torr at pH 7.5 in the presence of IHP (Shibayama et al., 1986b). After temperature correction (Rivetti et al., 1993a; Bettati et al., 1996, and see below), the oxygen affinity determined in solution is the same as in the crystal.

The temperature dependence of the oxygen affinity was measured between 5 and 20 °C. From the van't Hoff plot (Fig. 9), a ΔH of -11.5 ± 0.4 kcal/mol was calculated. The value of ΔH for $\alpha(\text{Ni}^{2+})_2\beta(\text{Fe}^{2+})_2$ crystals was -12.1 ± 0.8 kcal/mol (Bettati et al., 1996) and that for Hb A crystals was -13.3 ± 0.8 kcal/mol (Rivetti et al., 1993a).

Discussion

Oxygen binding curves of human hemoglobin A crystals exhibit a Hill coefficient of one both in the absence (Mozzarelli et al., 1991; Rivetti et al., 1993a) and in the presence of allosteric effectors

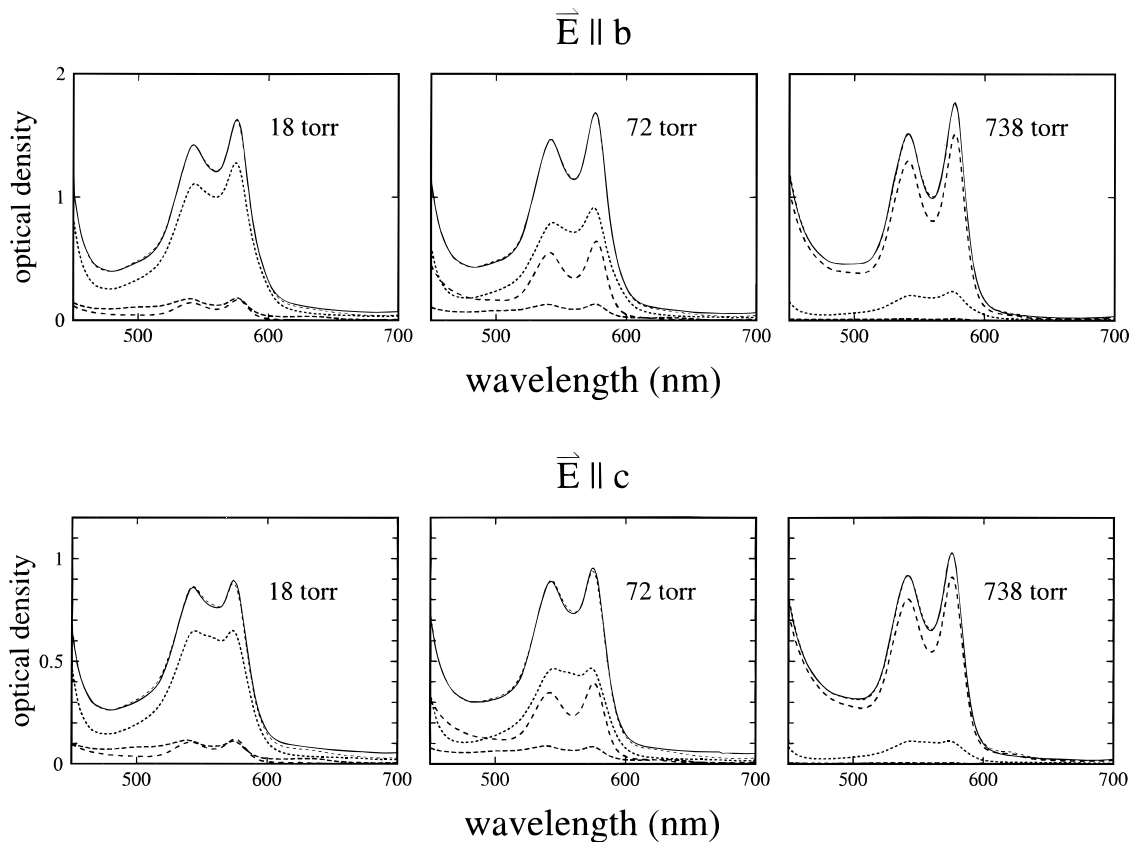


Fig. 3. Fit of the observed spectra (continuous curves) at different oxygen pressures with a linear combination of oxy, deoxy, and met reference spectra (dashed lines). The calculated best-fit spectrum is shown in each panel as the dashed curve that superimposes on the observed spectrum.

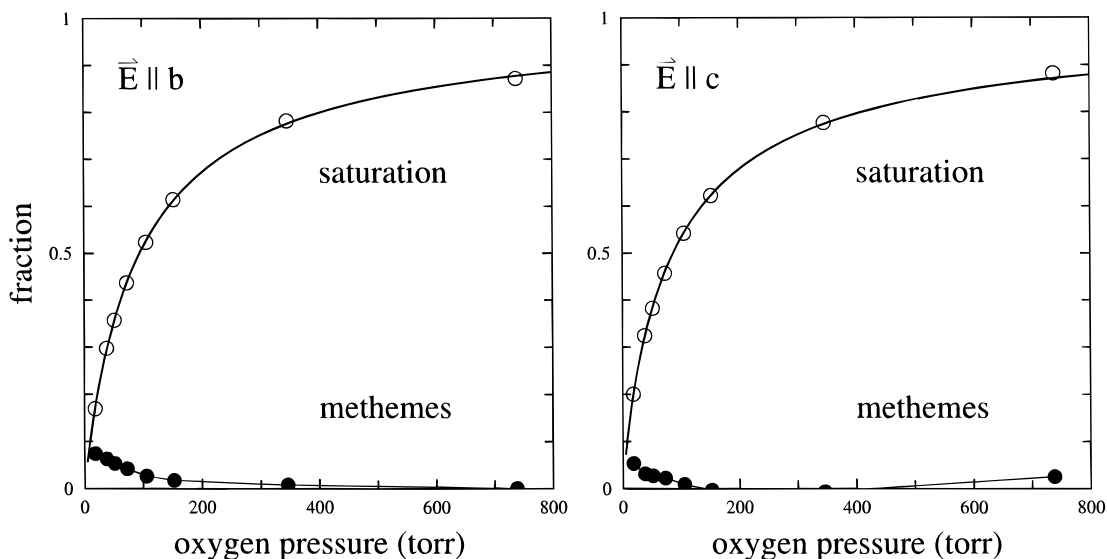


Fig. 4. Dependence of the fractional saturation with oxygen (open circles) of reduced hemes and the fraction of oxidized hemes (filled circles) as a function of oxygen pressure.

(Mozzarelli et al., 1997). The same finding was observed for hemoglobins modified at the $\alpha_1\beta_2$ subunit interface, Hb Rothschild (β Trp37Arg) (Rivetti et al., 1993b), at the α -subunit carboxy terminus, desArg141 α Hb (Kavanaugh et al., 1995) and at the β -subunit carboxy terminus, desHis146 β Hb (Bettati et al., 1997) and Hb Cowtown (β His146Leu) (Bettati et al., 1998). The oxygen affinities range from about 10 Torr for the desArg141 α Hb (Kavanaugh et al., 1995) to 140 Torr for Hb A (Rivetti et al., 1993a). The oxygen affinity of Hb in the crystal is the same in the absence and in the presence of IHP (Mozzarelli et al., 1997), indicating that crystallization has stabilized the lowest oxygen affinity T state. The same tertiary T state is obtained in solution in the presence of

strong allosteric effectors (Lalezari et al., 1990; Marden et al., 1990) and in metal hybrids containing magnesium (II) and zinc (II) (Miyazaki et al., 1999). Remarkably, the lowest oxygen affinity T state does not exhibit both a Bohr effect and IHP effect in solution (Miyazaki et al., 1999) as in the crystal (Rivetti et al., 1993a; Mozzarelli et al., 1997). Therefore, crystallization does not induce the formation of conformations not present in solution, only stabilizes one conformation over the others. Based on the model proposed by Rivetti et al. (1993a), suggesting that there are high and low oxygen affinity T states associated with broken and unbroken intersubunit salt bridges, the conformation stabilized in the crystal is that with intact salt bridges.

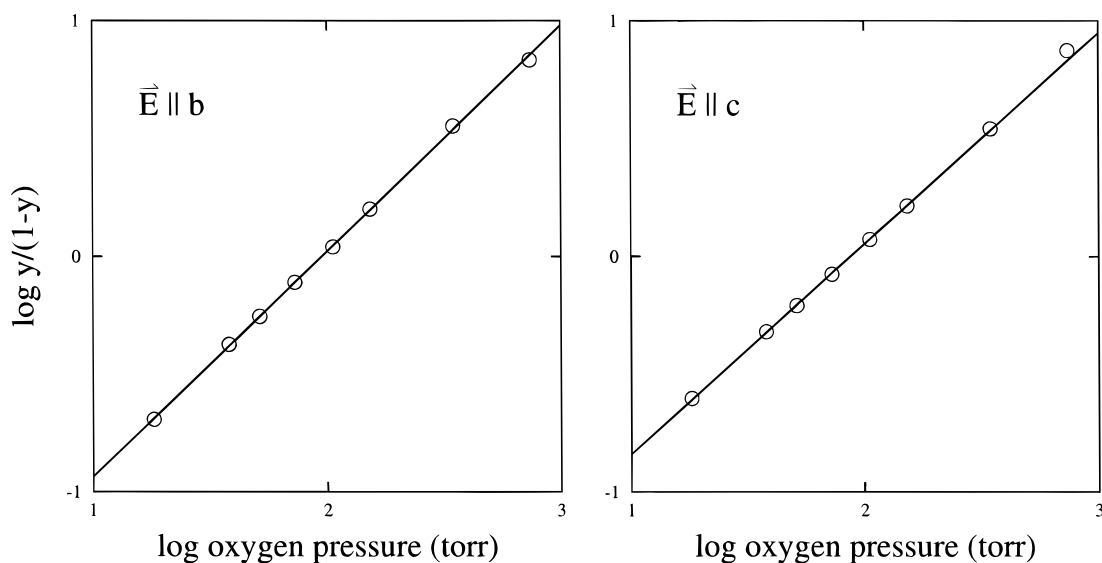


Fig. 5. Hill plot of the oxygen binding curves shown in Figure 5. The Hill coefficients and the p50s are 0.96 ± 0.03 and 93 ± 4 Torr, and 0.89 ± 0.02 and 85 ± 4 Torr along the *b* and *c* axes, respectively.

Table 2. Projections of heme planes used in calculations of $\alpha(\text{Fe}^{2+})_2\beta(\text{Ni}^{2+})_2$ crystals

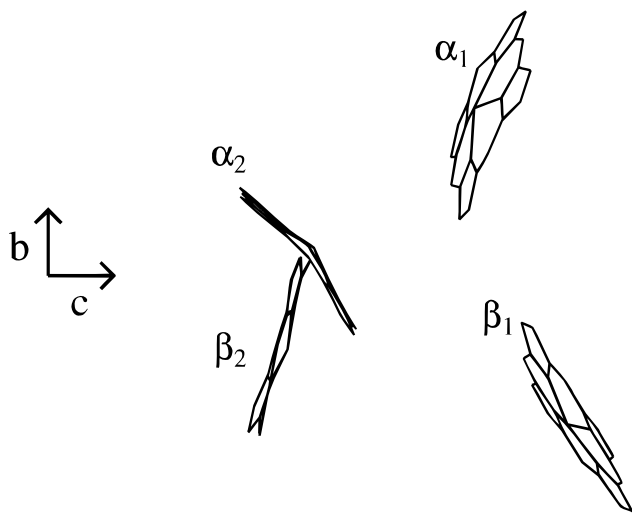
Hemoglobin	Subunit	$\sin^2 z_i a^*$	$\sin^2 z_i b$	$\sin^2 z_i c$
Deoxy ^a	α_1	0.947	0.886	0.167
	α_2	0.999	0.595	0.312
	β_1	0.972	0.716	0.407
	β_2	0.999	0.930	0.071
Oxy ^b	α_1	0.943	0.904	0.153
	α_2	0.996	0.576	0.428
	β_1	0.958	0.757	0.285
	β_2	0.995	0.939	0.066
Met ^c	α_1	0.955	0.897	0.148
	α_2	0.997	0.541	0.462
	β_1	0.976	0.665	0.358
	β_2	0.995	0.923	0.082

^aStructure reported in this paper. The submitted atomic coordinates are in the abc^* axis system, so it was necessary to transform the coordinates to the a^*bc axis system before computing the heme normal directions.

^bPDB file 1COH (T-state $\alpha(\text{FeCO})_2\beta(\text{Co})_2$ crystallized from PEG (Luisi & Shibayama, 1989)) oriented in the unit cell of the deoxyHb structure reported here.

^cPDB file 1HGB (T-state $\alpha(\text{Fe}^{3+})_2\beta(\text{Fe}^{3+})_2$ crystallized from PEG (Liddington et al., 1992)) oriented in the unit cell of the deoxyHb structure reported here.

A special feature of the optical measurements of hemoglobin crystals is that α and β hemes contribute differently to the polarized absorption spectra recorded along two perpendicular optical directions. Consequently, oxygen-binding curves measured along these directions differ to a certain degree reflecting the predominant projection of α or β hemes. To deconvolute the oxygen binding curves of the tetramer into the α and β heme oxygen binding curves, it is necessary to know the heme orientations in the deoxygenated and oxygenated states, and the relative contributions of α

**Fig. 6.** Projection of the iron-containing hemes of the α subunits and the nickel-containing hemes of the β subunits onto the bc crystal face of the polarized absorption measurements.

and β hemes to absorption intensity (Rivetti et al., 1993a). The calculated oxygen binding curves of α and β hemes indicated that the affinity of the α hemes was four to five times higher than the β hemes (Rivetti et al., 1993a). More recently, using a more complete set of structural data (Paoli et al., 1996), the deconvolution of the oxygen binding curves of the tetramer into the α and β heme oxygen binding curves was carried out for Hb A crystals in the presence of allosteric effectors (Mozzarelli et al., 1997). These calculations indicated that the α hemes exhibit an affinity 2.5 times higher than the β hemes, in good agreement with kinetic (Sawicki & Gibson, 1977), nuclear magnetic resonance (Lindstrom & Ho, 1972), electron paramagnetic resonance (Asakura & Lau, 1978), and thermodynamic (Shibayama et al., 1986a, 1986b) measurements on metal-hybrid hemoglobins. In the absence of any cooperativity, nonequivalent oxygen binding of α and β hemes leads to a Hill coefficient less than one. For example, a value of 0.89 is estimated for a fourfold affinity difference between α and β hemes (Rivetti et al., 1993a). These findings would imply that oxygen binding by T-state hemoglobin is characterized by a Hill coefficient slightly higher than one to result in the experimental value of unity observed for Hb crystals. On the basis of the calculated α - β inequivalence, the cooperativity of T state Hb is very low (Mozzarelli et al., 1997). However, this conclusion derives from a calculation of α and β heme affinities based on small differences in heme projections.

To experimentally define the oxygen affinity of α and β hemes, we have first investigated the oxygen binding by $\alpha(\text{Ni}^{2+})_2\beta(\text{Fe}^{2+})_2$ crystals (Bettati et al., 1996) and found that the average p50 of the β subunits is 110 Torr at 15 °C, a value about twofold smaller than the value calculated for β hemes (Mozzarelli et al., 1997). The p50s of the same hybrid, determined in solution in the absence and in the presence of PEG, are 71 and 80 Torr, respectively. In the present study, we have completed the evaluation of the oxygen affinity of α and β hemes by experimentally determining the p50 of the α hemes. The average value is 91 Torr. This indicates that the α hemes exhibit an oxygen affinity only about 1.2 times higher than the β hemes, a ratio very close to 1.3 found in solution in the presence of IHP at pH 7.5 (Shibayama et al., 1986b). The oxygen-binding curve of a hemoglobin tetramer containing α subunits with p50 of 91 Torr and β subunits with p50 of 110 Torr exhibits a Hill coefficient of 0.998 and an average p50 of 100 Torr. Consequently, the cooperativity of T-state Hb is even lower than that previously estimated (Bettati et al., 1996; Mozzarelli et al., 1997) and essentially negligible.

It may be argued (Ackers, 1998) that the crystal lattice constrains hemoglobin molecules, thus preventing functionally relevant tertiary conformational changes from taking place upon oxygen uptake within the α - β dimer of the tetramer in solution. The absence of the influence of allosteric effectors on oxygen affinity observed in the crystal and the absence of Bohr effect might be taken as evidence that Hb in the crystal is not a good system to learn about Hb function in solution. These criticisms would not only undermine the validity of our approach but also any X-ray crystallographic studies. In fact, if the crystal lattice forces protein molecules in conformations different from those present in solution, 3D structures have little to say on protein function in solution. Tertiary conformational changes associated to ligand binding have been detected by X-ray crystallography by comparing the structure of the unliganded and liganded Hb. These changes involve movements of the iron, the hemes, and amino acid residues. The observed tertiary conformational changes within the T state are along

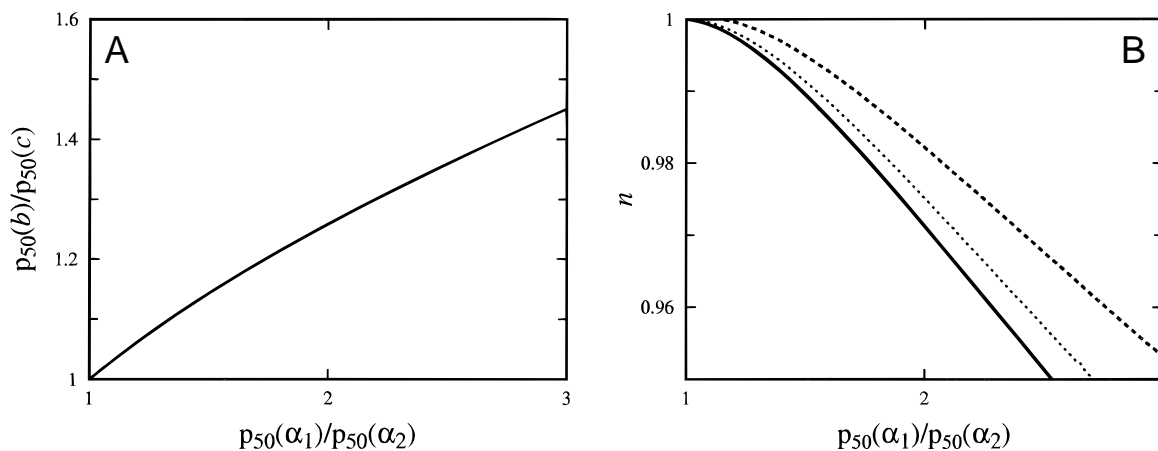


Fig. 7. Relation between apparent crystal binding curves and α -subunit binding curves for $\alpha(\text{Fe}^{2+})_2\beta(\text{Ni}^{2+})_2$ crystals. **A:** Dependence of the ratio of α_1 and α_2 heme affinities on the ratio of p_{50} s observed for light polarized along the b and c crystal axes. **B:** Hill n values observed for light polarized parallel to the b (heavy broken curve) and c (heavy solid line) crystal axes, and the isotropic average (light broken curve), as a function of the ratio of α_1 and α_2 heme affinities.

the structural pathway from the deoxy T to the oxy R (Liddington et al., 1992; Paoli et al., 1996). In agreement with the structural data, the polarization ratio, a parameter very sensitive to heme tilt, was found to vary from deoxy to oxy and metHb (Rivetti et al., 1993a). Furthermore, protein dynamics and function in the crystal have usually been found to be the same as in solution (Mozzarelli & Rossi, 1996; Mozzarelli & Bettati, 2000; and references therein). An interesting example is the oxygen binding by *Scapharca inaequalvis* HbI, a hemoglobin in which the mechanism of cooperativity is mainly based on tertiary conformational changes (Royer et al., 1989, 1990). It was found that *Scapharca inaequalvis* HbI crystals (Mozzarelli et al., 1996) bind oxygen with the same cooperativity (Hill $n = 1.4$) and affinity ($p_{50} = 4.9$ Torr) as in solution.

The two α hemes bind oxygen with slightly different affinities, as previously observed for the two β hemes (Bettati et al., 1996).

Structural inequivalence between the two α hemes in the crystal may arise from packing of the tetramers in the $P2_1$ monoclinic lattice, which provides structurally nonequivalent environments to the subunits. In particular, whereas the α_1 heme propionate groups point roughly toward the β_1 N-terminal region of a symmetry-related Hb tetramer, the α_2 heme propionates face the distal-site region of a symmetry-related β_2 chain. Such molecular packing differences may account for different kinetics of ligand diffusion to the α hemes in the crystal, but may also exert some influence on the structural/dynamic rearrangements of the individual α chains in their reaction with oxygen. Indeed, different occupancies with oxygen were observed for the two α subunits of liganded $\alpha(\text{Fe}^{2+}\text{O}_2)_2\beta(\text{Ni}^{2+})_2$ crystals and were attributed to different crystal contacts of the α subunits (Luisi & Shibayama, 1989). Detailed inspection of the heme cavities shows that both α hemes are slightly

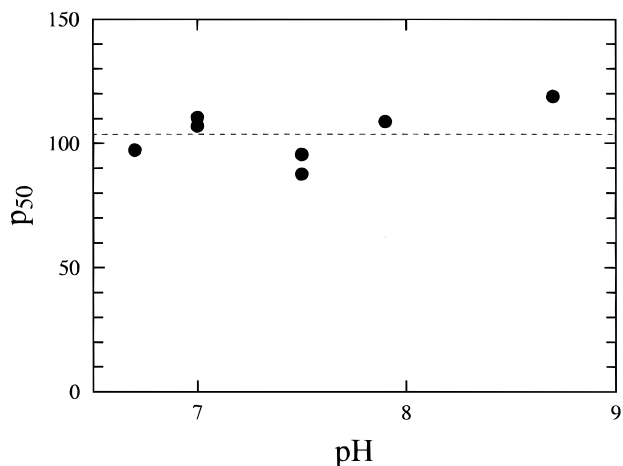


Fig. 8. Dependence of the oxygen affinity on pH. Oxygen binding curves were determined for crystals suspended in solutions containing 50% (w/v) PEG 1000, 10 mM potassium phosphate, 1 mM IHP, at different pH values, 15 °C. The p_{50} is the mean of the values determined along the b and c axes.

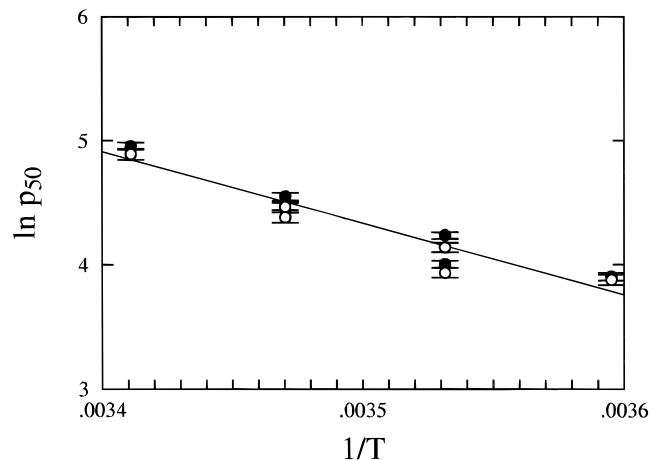


Fig. 9. Dependence of the oxygen affinity on temperature. Oxygen binding curves were determined for crystals suspended in a solution containing 50% (w/v) PEG 1000, 10 mM potassium phosphate, 1 mM IHP, pH 7.5. The values of p_{50} were determined from experiments using light polarized along the b (filled circles) and c (open circles) axes.

domed along the CHA-CHC methine-bridge axis. An overlay of the C α backbones of both α chains yields an RMSD of 0.30 Å (calculated over 141 atom pairs). Inspection of the superimposed structures in the protein region surrounding the heme group does not reveal any structural difference between the two α hemes within the estimated experimental error.

Finally, the absence of a Bohr effect in $\alpha(\text{Fe}^{2+})_2\beta(\text{Ni}^{2+})_2$ crystals, and in all other Hbs examined in the crystalline state, is in keeping with the absence of structural changes of the groups of both α and β subunits predominantly involved in the Bohr effect (Perutz, 1970), as crystallographically documented in the liganded hybrids (Luisi & Shibayama, 1989; Luisi et al., 1990) and in all other liganded Hbs (Arnone et al., 1986; Abraham et al., 1992; Liddington et al., 1992; Paoli et al., 1996). Thus, crystallization stabilizes Hb in the lowest affinity T state where ligand binding does not lead to salt bridge breakage (Miyazaki et al., 1999).

Materials and methods

Preparation of crystals

The hemoglobin metal hybrid $\alpha(\text{Fe}^{2+})_2\beta(\text{Ni}^{2+})_2$ was prepared and purified using a modified version of the method of Shibayama et al. (1986a). Samples were stored at -80°C in a CO-saturated environment. CO was removed by photolysis in a stream of humidified oxygen at 4°C . Crystals were grown from a deoxygenated solution containing 24 mg/mL hybrid hemoglobin and 21% (w/v) PEG 1000 (Hampton Research, Riverside, California), 10 mM potassium phosphate, 1 mM inositol hexaphosphate (IHP), 30 mM sodium dithionite, pH 7, at room temperature. Crystals appeared after 24–48 h. After growth, crystals were first resuspended twice in a solution containing 35% (w/v) PEG 1000, 10 mM potassium phosphate, 1 mM IHP, and 30 mM sodium dithionite at pH 7.5, and twice in a solution of the same composition but 50% (w/v) PEG 1000. Crystals were stored under anaerobic conditions at 20°C . No crystal damage was observed upon exposure to oxygen.

X-ray diffraction data collection of deoxy $\alpha(\text{Fe}^{2+})_2\beta(\text{Ni}^{2+})_2$ crystals

Prior to X-ray exposure a batch of five suitable crystals was removed from the anaerobic storage buffer, and washed twice with a 50% (w/v) PEG 1000 solution, 10 mM sodium phosphate, containing 30 mM potassium dithionite and 1 mM IHP at pH 7.5. The crystal selected for data collection was flash frozen under a nitrogen gas stream at 100 K and used for X-ray data collection on a Rigaku R-axis IIC image plate system, using Cu K α radiation. Under these experimental conditions, diffraction data to a minimum spacing of 2.1 Å could be collected (see Table 3; evident crystal decay prevented data collection at room temperature). Diffraction data reduction was achieved using MOSFLM and programs from the CCP4 program suite (Bailey, 1994).

Crystals of $\alpha(\text{Fe}^{2+})_2\beta(\text{Ni}^{2+})_2$ are essentially isomorphous with those obtained by Luisi and Shibayama (1989) for deoxy $\alpha(\text{Fe}^{2+})_2\beta(\text{Co}^{2+})_2$ (PDB entry 1COH) and the carbonmonoxy adduct $\alpha(\text{Ni}^{2+})_2\beta(\text{FeCO})_2$ (PDB entry 1NIH), grown from ammonium sulfate solutions. The atomic coordinates of these hybrids were used as the starting model for the present crystallographic refinement. Since the unit cell edges of $\alpha(\text{Fe}^{2+})_2\beta(\text{Ni}^{2+})_2$ (this study) were indexed differently from those of Luisi and Shibayama

Table 3. Crystallographic data

Space group: monoclinic P2 ₁	
Unit cell: $a = 55.7$, $b = 81.4$, $c = 63.1$ Å, $\alpha = \gamma = 90^\circ$, $\beta = 97.8^\circ$	
$V_M = 2.28$ Å ³ /Da (one Hb tetramer per asymmetric unit)	
Resolution range: 22.4–2.1 Å	
Independent reflections: 32,068	
Completeness: 98%	
R-merge : 6%	

RMSDs for stereochemical parameters of the refined model

R-factor (12.0–2.1 Å)	20.0%
R_{free} (5% of the data)	28.0%
Cruickshank DPI	0.28 Å
Ramachandran outliers	None
RMSD bond lengths	0.018 Å
RMSD bond angles	0.040 Å
RMSD planar groups	0.046 Å
Average B-factor	
Protein backbone	24.8 Å ²
Side chains	45.6 Å ²

(1989) by an interchange of the a and c axes (see Table 3), a preliminary molecular replacement search, run with the program AmoRe (Bailey, 1994), allowed proper reorientation of the Hb tetramer (the correlation coefficient for the molecular replacement solution was 54.9). After rigid body refinement of the starting model, the R -factor was 0.361, in the 15–3.0 Å resolution range (correlation coefficient 71.2).

The 3D structure of the $\alpha(\text{Fe}^{2+})_2\beta(\text{Ni}^{2+})_2$ tetramer was subsequently refined using the REFMAC program for restrained crystallographic refinement applying a bulk solvent correction (Murshudov et al., 1997), in conjunction with the molecular graphics program O (Jones et al., 1991). The final model, which includes 4,380 protein atoms, four porphyrin groups, 2 Fe²⁺, 2 Ni²⁺, and 266 water molecules, displays ideal stereochemical parameters (see Table 3), with a general R -factor value of 20.0% ($R_{\text{free}} = 28.0\%$), for the data in the 12.0–2.1 Å resolution range.

Microspectrophotometric measurements

Before measurements, crystals were resuspended six times in a solution containing 50% (w/v) PEG 1000, 10 mM potassium phosphate, 1 mM IHP, at a defined pH, and loaded in a Dvorak–Stotler flow cell (Dvorak & Stotler, 1971), as previously described (Rivetti et al., 1993a). Single crystal polarized absorption spectra were determined as a function of oxygen pressure by a system including a Zeiss MPM03 microspectrophotometer, a gas mixer generator (Envionics, series 200) and an oxygen meter, equipped with a Clark electrode (Yellow Spring), calibrated with humidified helium, oxygen, and 5 and 21% oxygen mixtures. The electric vector of the incident light was parallel to either the b or the c crystal axis. Fractional saturations of reduced hemes with oxygen and fractions of oxidized hemes were calculated by fitting the observed spectra to a linear combination of the spectra of the fully deoxy, oxy, and oxidized Hb crystals (reference spectra; Fig. 10) (Rivetti et al., 1993a). The spectra of deoxy metal-hybrid Hb crystals were obtained by resuspending crystals in a solution containing 30 mM dithionite, 10 mM potassium phosphate, 50% (w/v) PEG 1000,

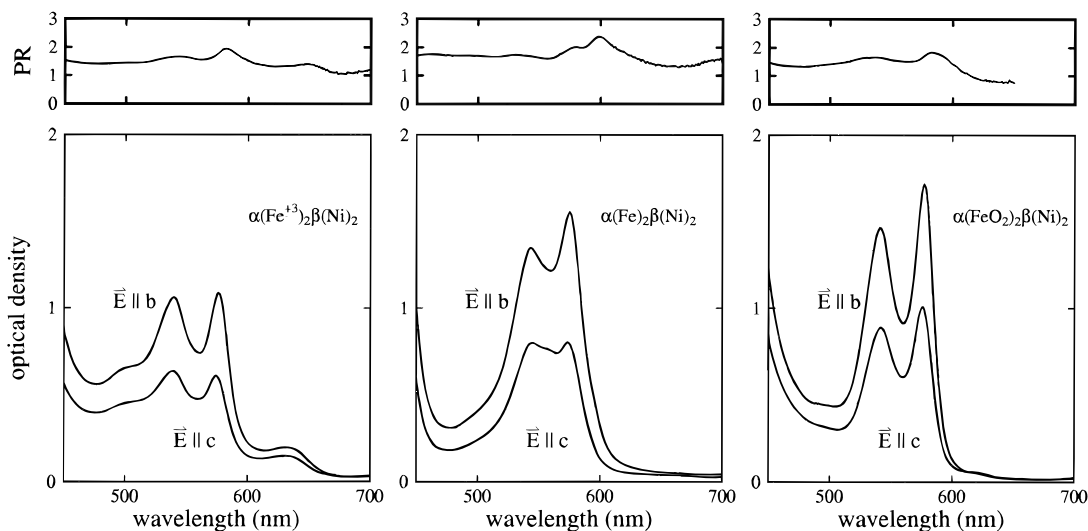


Fig. 10. Polarized absorption spectra (reference spectra) and polarization ratios (PR) of fully oxidized, reduced, and oxygenated $\alpha(\text{Fe}^{2+})_2\beta(\text{Ni}^{2+})_2$ crystals. The band shape is affected by the absorption properties of the nonoxygen binding nickel porphyrins of the β subunits.

pH 7. The same crystal was resuspended in a dithionite-free solution and, then, in a solution containing 5 mM potassium ferricyanide. Upon complete oxidation, evaluated by the increase of the peak at 630 nm, crystals were resuspended in a solution containing 50% (w/v) PEG 1000, 10 mM potassium phosphate, 1 mM IHP. Spectra of the oxidized metal hybrid crystals were collected as a function of pH. Spectra of fully oxygenated metal-hybrid crystals were obtained by recording spectra at different oxygen pressures between 160 and 760 Torr, at 5 °C, and by extrapolating the series of spectra to infinite oxygen pressure (Rivetti et al., 1993a).

Measurements carried out at 20 °C are affected by a relatively higher rate of heme oxidation than at lower temperature (8 and 3% of metHb formation in 300 min, at 20 and 15 °C, respectively). This faster rate of oxidation and the appearance of a new species absorbing at ~550 nm, attributed to a hemichrome, prevented the determination of a complete binding curve on the same crystal.

Acknowledgments

We thank Dr. William A. Eaton and Prof. Gian Luigi Rossi for helpful discussions and critical readings of the manuscript. This work has been supported by a NATO Collaborative Research Grant (to A.M. CRG.930826) and in part by funds from the National Research Council of Italy (to A.M. 98.01117.CT14; the Target Project on Biotechnology) and the Ministry of University and Scientific and Technological Research of Italy. Support was also provided by a research grant from the National Heart, Lung, and Blood Institute (to T.Y. HL14508).

References

- Abraham DJ, Peascoe RA, Randad RS, Panikker J. 1992. X-ray diffraction study of di-ligated and tetra-ligated T-state hemoglobin from high salt crystals. *J Mol Biol* 227:480–492.
- Ackers GK. 1998. Deciphering the molecular code of hemoglobin allostery. *Adv Prot Chem* 51:185–253.
- Ackers GK, Doyle ML, Myers DM, Daugherty MA. 1992. Molecular code for cooperativity in hemoglobin. *Science* 255:54–63.
- Arnone A, Rogers P, Blough N, McGourty J, Hoffman B. 1986. X-ray diffraction studies of a partially liganded hemoglobin, $[\alpha(\text{FeII-CO})\beta(\text{MnII})]_2$. *J Mol Biol* 188:693–706.
- Asakura T, Lau PW. 1978. Sequence of oxygen binding by hemoglobin. *Proc Natl Acad Sci USA* 75:5462–5465.

- Bailey S. 1994. The CCP4 suite—Programs for protein crystallography. *Acta Crystallogr Sect D* 50:760–763.
- Bettati S, Kwiatkowski LD, Kavanaugh JS, Mozzarelli A, Arnone A, Rossi GL, Noble RW. 1997. Structure and oxygen affinity of crystalline desHis146 β human hemoglobin in the T state. *J Biol Chem* 272:33077–33084.
- Bettati S, Mozzarelli A. 1997. T state hemoglobin binds oxygen noncooperatively with allosteric effects of protons, inositol hexaphosphate, and chloride. *J Biol Chem* 272:32050–32055.
- Bettati S, Mozzarelli A, Perutz MF. 1998. Allosteric mechanism of haemoglobin: Rupture of salt-bridges raises the oxygen affinity of the T structure. *J Mol Biol* 281:581–585.
- Bettati S, Mozzarelli A, Rivetti C, Rossi GL, Tsuneshige A, Yonetani T, Eaton WA, Henry ER. 1996. Oxygen binding by single crystals of hemoglobin: The problem of cooperativity and inequivalence of alpha and beta subunits. *Proteins* 25:425–437.
- Brzozowski A, Derewenda Z, Dodson E, Dodson G, Grabowski M, Liddington R, Skarzynski T, Valley D. 1984. Bonding of molecular oxygen to T state human haemoglobin. *Nature* 307:74–76.
- Dvorak JA, Stotler WF. 1971. A controlled-environment culture system for high resolution light microscopy. *Exp Cell Res* 68:144–148.
- Eaton WA, Henry ER, Hofrichter J, Mozzarelli A. 1999. Is cooperative oxygen binding by hemoglobin really understood? *Nat Struct Biol* 6:351–358.
- Haurowitz F. 1938. Das Gleichgewicht zwischen Hämoglobin und Sauerstoff. *Hoppe-Seyler Z Physiol Chem* 254:266–274.
- Jones TA, Zou JY, Cowan SW, Kjeldgaard M. 1991. Improved methods for building protein models in electron-density maps and the location of errors in these models. *Acta Crystallogr Sect A* 47:110–119.
- Kavanaugh JS, Chafin DR, Arnone A, Mozzarelli A, Rivetti C, Rossi GL, Kwiatkowski LD, Noble RW. 1995. Structure and oxygen affinity of crystalline desArg141 α human hemoglobin A in the T state. *J Mol Biol* 248:136–150.
- Koshland DE, Nemethy G, Filmer D. 1966. Comparison of experimental binding data and theoretical methods in proteins containing subunits. *Biochemistry* 5:365–385.
- Lalezari I, Lalezari P, Poyart C, Marden MC, Kister J, Bohn B, Fermi G, Perutz MF. 1990. New effectors of human hemoglobin: Structure and function. *Biochemistry* 29:1515–1523.
- Lee A, Karplus M, Poyart C, Bursaux E. 1988. Analysis of proton release in oxygen binding by hemoglobin: Implications for the cooperative mechanism. *Biochemistry* 27:1285–1301.
- Liddington R, Derewenda Z, Dodson G, Harris D. 1988. Structure of the liganded T state of haemoglobin identifies the origin of cooperative oxygen binding. *Nature* 331:725–728.
- Liddington R, Derewenda Z, Dodson E, Hubbard R, Dodson G. 1992. High-resolution crystal-structures and comparisons of T-state deoxyhaemoglobin and two liganded T-state haemoglobins: T(α -oxy)haemoglobin and T(met)haemoglobin. *J Mol Biol* 228:551–579.
- Lindstrom TR, Ho C. 1972. Functional nonequivalence of α and β hemes in human hemoglobin. *Proc Natl Acad Sci USA* 69:1707–1710.

- Luisi B, Liddington B, Fermi G, Shibayama N. 1990. Structure of deoxy-quaternary hemoglobin with liganded β subunits. *J Mol Biol* 214:7–14.
- Luisi B, Shibayama N. 1989. Structure of hemoglobin in the deoxy quaternary state with ligand bound at the α haems. *J Mol Biol* 206:723–736.
- Marden MC, Bohn B, Kister J, Poyart C. 1990. Effectors of hemoglobin: Separation of allosteric and affinity factors. *Biophys J* 57:397–403.
- Miyazaki G, Morimoto H, Yun K-M, Park S-Y, Nakagawa A, Minagawa H, Shibayama N. 1999. Magnesium(II) and zinc(II)-protoporphyrin IX's stabilize the lowest oxygen affinity state of human hemoglobin even more strongly than deoxyheme. *J Mol Biol* 292:1121–1136.
- Monod J, Wyman J, Changeux J-P. 1965. On the nature of allosteric transitions: A plausible model. *J Mol Biol* 12:88–118.
- Mozzarelli A, Bettati S. 2000. Functional properties of immobilized proteins. In: *Advanced functional molecules and polymers*. Tokyo: Gordon and Breach Science Publishers. Forthcoming.
- Mozzarelli A, Bettati S, Rivetti C, Rossi GL, Colotti G, Chiancone E. 1996. Cooperative oxygen binding to *Scapharca inaequivalvis* hemoglobin in the crystal. *J Biol Chem* 271:3627–3632.
- Mozzarelli A, Rivetti C, Rossi GL, Eaton WA, Henry ER. 1997. Allosteric effectors do not alter the oxygen affinity of hemoglobin crystals. *Protein Sci* 6:484–489.
- Mozzarelli A, Rivetti C, Rossi GL, Henry ER, Eaton WA. 1991. Crystals of hemoglobin with the T quaternary structure bind oxygen noncooperatively with no Bohr effect. *Nature* 351:416–419.
- Mozzarelli A, Rossi GL. 1996. Protein function in the crystal. *Annu Rev Biophys Biomol Struct* 25:343–365.
- Murshudov GN, Vagin AA, Dodson EJ. 1997. Refinement of macromolecular structures by the maximum-likelihood method. *Acta Cryst Sect D* 53:240–255.
- Paoli M, Liddington R, Tame J, Wilkinson A, Dodson G. 1996. Crystal structure of T state haemoglobin with oxygen bound at all four haems. *J Mol Biol* 256:775–792.
- Pauling L. 1935. The oxygen equilibrium of hemoglobin and its structural interpretation. *Proc Natl Acad Sci USA* 21:186–191.
- Perutz MF. 1970. Stereochemistry of cooperative effects in haemoglobin. *Nature* 228:726–739.
- Perutz MF. 1989. Mechanisms of cooperativity and allosteric regulation in proteins. *Quart Rev Biophys* 22:139–236.
- Perutz MF, Wilkinson A, Paoli M, Dodson G. 1998. The stereochemical mechanism of the cooperative effects in hemoglobin revisited. *Annu Rev Biophys Biomol Struct* 27:1–34.
- Rivetti C, Mozzarelli A, Rossi GL, Henry ER, Eaton WA. 1993a. Oxygen binding by single crystals of hemoglobin. *Biochemistry* 32:2888–2906.
- Rivetti C, Mozzarelli A, Rossi GL, Kwiatkowski LD, Wierzbka A, Noble RW. 1993b. Effect of chloride on oxygen binding to crystals of hemoglobin Rothschild ($\beta 37$ Trp \rightarrow Arg) in the T quaternary structure. *Biochemistry* 32:6411–6418.
- Royer WE, Hendrickson WA, Chiancone E. 1989. The 2.4-Å crystal-structure of *Scapharca* dimeric hemoglobin—Cooperativity based on directly communicating hemes at a novel subunit interface. *J Biol Chem* 264:21052–21061.
- Royer WE, Hendrickson WA, Chiancone E. 1990. Structural transitions upon ligand binding in a cooperative dimeric hemoglobin. *Science* 249:518–521.
- Sawicki CA, Gibson QH. 1977. Properties of the T state of human oxyhemoglobin studied by laser photolysis. *J Biol Chem* 252:7538–7547.
- Shibayama N, Morimoto H, Kitagawa T. 1986a. Oxygen equilibrium study and light absorption spectra of Ni(II)-Fe(II) hybrid hemoglobins. *J Mol Biol* 192:322–329.
- Shibayama N, Morimoto H, Kitagawa T. 1986b. Properties of chemically modified Ni(II)-Fe(II) hybrid hemoglobins. Ni(II) protoporphyrin IX as a model for a permanent deoxy-heme. *J Mol Biol* 192:331–336.
- Shibayama N, Morimoto H, Saigo S. 1997. Reexamination of the hyper thermodynamic stability of asymmetric cyanomet valency hybrid hemoglobin ($\alpha^{+CN}\beta^{+CN}$)($\alpha\beta$): No preferentially populating asymmetric hybrid at equilibrium. *Biochemistry* 36:4375–4381.
- Shibayama N, Morimoto H, Saigo S. 1998. Asymmetric cyanomet valency hybrid hemoglobin, ($\alpha^{+CN}\beta^{+CN}$)($\alpha\beta$): The issue of valency exchange. *Biochemistry* 37:6221–6228.
- Shibayama N, Saigo S. 1995. Fixation of the quaternary structures of human adult hemoglobin by encapsulation in transparent porous silica gels. *J Mol Biol* 251:203–209.
- Sun DZP, Zou M, Ho NT, Ho C. 1997. Contribution of surface histidyl residues in the α -chain to the Bohr effect of human normal adult hemoglobin: Roles of global electrostatic effects. *Biochemistry* 36:6663–6673.